ANNUAL OF NAVIGATION 1/99

Jarosław Artyszuk
Maritime University
Szczecin

DYNAMICS - BASED IDENTIFICATION OF SHIP MOTION MATHEMATICAL MODEL FROM FULL-SCALE TRIALS RESULTS

ABSTRACT

A new identification technique of ship's dynamics for integrated navigational systems is proposed. It is derived from motion equations analysis. The major attraction is differentiation-based gathering of exciting forces during manoeuvres and thus model validation on the lowest level.

1. INTRODUCTION

1.1. The concept formulation

Integrated navigational systems (INSs) are designed to perform plenty tasks, of which part is being accomplished through an extensive use of the ship motion mathematical model.

These functions generally comprise:

- manoeuvres simulation (decision-making process support),
- automatic control of ship's motion over requested trajectory - case of dynamic positioning and unmanned manoeuvring (execution process support),
- state vector estimation in filtering units - navigational data processing to support both former functions.

The main highlight of an integrated system is that it is developed (tuned) for a particular ship, which behavior was already assessed during delivery trials (obligatory in full scale)

The most common approach in the identification of ship motions mathematical models, or in other words, in the tuning of simulation models parameters as to reach an arbitrary behavior, is the kinematics-related one. Its main objective is to achieve a proper validation of the final curves of motion variables (of displacement or velocity types). But there is an imminent danger, that the expected motion is arrived at with improper parameters (ambiguity) or inaccurate values thereof (low sensitivity), despite the fact it is sometimes very hard to find those "responsible parameters". A quite different aspect is the impossibility of getting close to trial results due to inherent errors in the trials themselves, what is not often so evident.

All before mentioned difficulties seem to be cleared up by the dynamics (force) based special identification procedure. It warrants also the model validation on lowest possible level and thus its higher reliability. The problem is known, but the manner of its solution, i.e. the identification scheme is rather a new attitude towards an identification process.

1.2. Differentiation technique

The fundamental basis of hereafter analysis is a numerical differentiation of an experimental variable given in a form of table.

It is assumed, that variable being considered "x" is tabulated at constant intervals of independent variable, e.g. time "t":

$$x_0, x_1, x_2, \ldots, x_n,$$

where: $x_k = f(t_k)$, k= 0, 1, 2,..., n;

$$t_{k+1} = t_k + \Delta t \text{ , } \Delta t = const.$$

If the condition $\Delta t = const$ is not fulfilled, it could be easy reached by simple linear interpolation of x against appropriate fixed time values.

The derivative looks then like:

$$\left.\frac{dx}{dt}\right|_{t_k} = \frac{x_{k+1} - x_{k-1}}{2\Delta t}, \; k = 1, 2, \ldots, n\text{-}1, \tag{1}$$

where $\left.\frac{dx}{dt}\right|_{t_0}$ is taken from initial conditions (for accelerations nearly always 0).

Upon completion of the derivative calculation, it is necessary to smooth its values for original data inherent errors and time discretization (i.e. method error). There is no general rule for this process, which should be based on experience and knowledge of a typical, visual curve shape of the derivative. What regards the manoeuvring data (e.g. drift angle or yaw rate in turning test) is that it is very hard to find a universal analytical function which fits very well (mean square method) the data in any case. The another criterion used in the fairing stage is to achieve, on a satisfactory level (e.g. <5%), the original data x_k after integration (trapezoidal rule) applied to the derivative. Throughout this study only the latter criterion will be used, while the mean square approximation is left for further research.

Very important remark is due in this context. Namely it is dangerous to use the "ready-to-use" formula for the derivative:

$$\left.\frac{dx}{dt}\right|_{t_k} = 2\left(\frac{x_k - x_{k-1}}{\Delta t}\right) - \left.\frac{dx}{dt}\right|_{t_{k-1}}, \; k = 1, 2, \ldots, n. \tag{2}$$

It causes big oscillations (due to cumulative error) of final values and thus difficulty in exploring "an average run", see Fig. 1.

Fig. 1 shows effect of both methods (1) and (2), applied to the DGPS derived pure distance over track in a turning circle (time interval 5 sec.). One receives this way a total speed over ground indication (at antenna position). In Fig. 1, for comparison purposes, is also included an originally calculated speed (i.e. with filtering inertia). This one is a bit higher during an evolutionary phase of circulation.

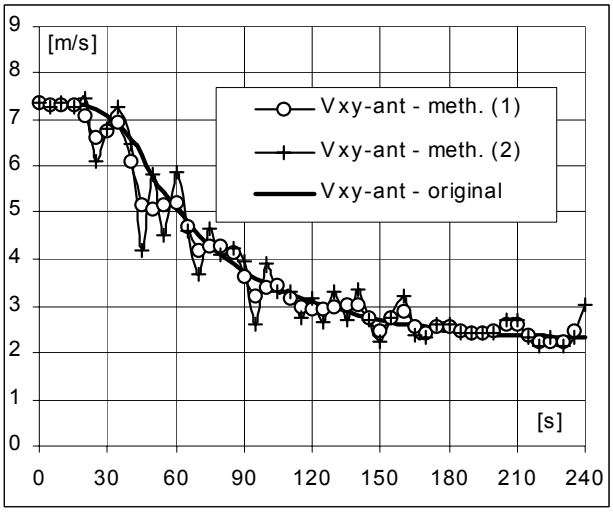

Fig.1. Numerical differentiation errors

It is commonly known, that differentiation in extreme cases (especially low time interval) can seriously reduce accuracy of the final derivative as compared to the original variable (see also [Ralston, 1983]).

Though one could claim, that 5s interval is too short, following example is helpful. Let the ship move at 5m/s. She covers in 5s a distance of 25m. If the distance is measured with DGPS accuracy ±2m at both ends, one gets speed 4.2÷5.8m/s. But if the speed is too low in one step, it will be increased1 in the next one. We are interested more in total (average) speed change then in its local behavior. The same applies also to graphically acquired data, as it is the case in our study, from available only manoeuvring charts.

1.3. Data source

The most powerful source of full-scale manoeuvring information is still shipyard's database. Trials are conducted as part of delivery stage of manufacturing, using own resources or supported more or less by external, independent centers. The latter happens recently, when high accuracy is required and lack of time is present. This also contributes into general growth of reliability of such trials.

The sea trials results are often of doubtful quality for different reasons. Primary, they are evaluated and presented for commercial purposes, which does not necessary mean time and money consuming high accuracy and complete trial report, required in scientific applications. Also, all factors affecting the experiment are seldom mentioned, what could allow a verification of the data and fully identify the motion. This prevents in some way development of motion mathematical model for existing ships, where the model behavior has boundaries, i.e. must fall into trial results (often colliding each other) for some tests.

Because in this paper, a motion mathematical model without current/wind effect is considered, selection of trials should also examine, in addition to comprehensive, reliable information, whether the ship during trial is affected significantly by both weather factors.

In this context, it is obvious that not every trial data is appropriate for present investigation, where rather high accuracy of initial data is of major concern for subsequent computations. Though it is possible to estimate quality of trials by means of wind force value prevailed during measurements, but this should be treated carefully. Because, relatively high wind forces do not affect deeply loaded ships and the current effect is mostly unknown. When relevant data are supplied, individual approach seems to ensure good selection of trials.

1.4. Full scale ship characteristics

Particulars of a full-scale ship selected into the investigation are collected in Table 1.

Table 1. Ship's particulars

TYPE: chemical tanker			WORKING CONDITIONS (own calculations)		
HULL			w	=	0.4014
L_{PP}	=	97.4m	t	=	0.2
B_M	=	16.6m	c_{Fxh}	=	-0.01496 ($L_{PP}T_M$ related, resistance coeff.)
T_M	=	7.1m	v_{FAH}	=	7.449m/s
c_B	=	0.7605	Q_D=95%$Q_{nM/E}$	=	223.69kNm (max. delivered torque)
m	=	8950t	RUDDER		
PROPULSION			type:		Schilling's
- M/E:			A_R	=	12.26m^2
type:		diesel	Λ_R	=	1.509
P_n	=	3600kW	OTHERS		
n_n	=	146rpm	Δa	=	-28.45m (antenna midship offset)
- PROPELLER:			J_z	=	5.158·10^6[tm^2] (ship's inertia moment)
type:		CPP			
D	=	4.1m	remark: all symbols mostly conform to "ITTC Symbols and		
P/D	=	0.8719	Terminology List", ver.1996		
A_E/A_0	=	0.52			
z	=	4			

Manoeuvring data for starboard turning circle (35º/FAH) is shown in Fig. 2 (marks show discretization points).

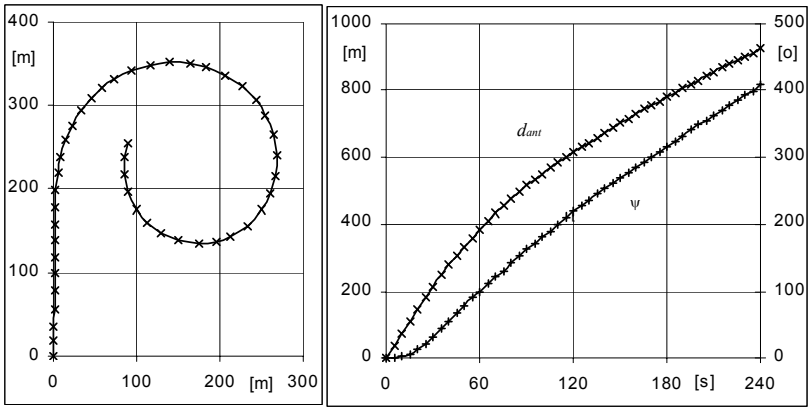

Fig. 2. Manoeuvring data

All measurements were automatically recorded. Track of antenna $x_{ant}=f(y_{ant})$ and its distance $d_{ant}=f(t)$ are based on the DGPS, while course (is derived from gyro.

They describe sufficiently the motion. The Variable d_{ant} was chosen instead of $v_{xy\text{-}ant}$ for reasons in Fig.1. All of the charts were digitized for computational purposes.

During trials, the wind was 7m/s (4ºB), but of less effect on the ship. As compared to a calm weather, the ship gains (for aft wind) or loses (for head wind) averagely 0.21kt proceeding at a reference speed of abt. 14kt. And due to the fact, that this one is reflected in a decrease (increase) of main engine power consumption, the current must be absent (at least in a wind direction). For the above reasons, we can assume no wind/current effect in the trials.

2. FORCE IDENTIFICATION

2.1. Ship motions equations

Let's introduce for our convenience simplified ship-fixed motions equations in a horizontal plane (conventions as used in [Artyszuk, 1998]), written as follows:

$$\begin{cases} (m+m_{11})\dfrac{dv_x}{dt} - (m+m_{22})v_y\omega_z = F_x \\ (m+m_{22})\dfrac{dv_y}{dt} + (m+m_{11})v_x\omega_z = F_y \\ (J_{zz}+m_{66})\dfrac{d\omega_z}{dt} + (m_{22}-m_{11})v_x v_y = M_{Az} \end{cases}, \qquad (3)$$

2.2. Velocities identification at antenna position

From earth coordinates of antenna position (Fig. 2):

$$(x_0,y_0)_{\text{ant}},\ (x_1,y_1)_{\text{ant}},\ldots,\ (x_n,y_n)_{\text{ant}};$$

Distance over track is calculated $d_{ant\text{-}c}$ (for reference only) and φ_{ant} (Fig. 3). Keeping in mind the "*ant*" subscript, the expressions read (k=1, 2,..., n–1):

$$\begin{cases} d_0 = d\big|_{y_0} = 0 \\ d_k = d_{k-1} + \sqrt{(y_k - y_{k-1})^2 + (x_k - x_{k-1})^2} \end{cases},$$

$$\begin{cases} \varphi_0 = \varphi\big|_{d_0} = 0 \\ \varphi_k = \operatorname{arctg}\left(\dfrac{dy}{dx}\Big|_{d_k} \right) = \dfrac{y_{k+1} - y_{k-1}}{x_{k+1} - x_{k-1}} \end{cases}.$$

Using function d_{ant}(t) (see Fig. 2), the next step is to convert:

$$\varphi(d_{ant-c}) \xrightarrow{d_{ant}(t)} \varphi(t).$$

After differentiation of d_{ant} and ψ:

$$v_{xy-ant} = \frac{d(d_{ant})}{dt}, \quad \omega_{z-ant} = \frac{d\psi}{dt},$$

all velocities (at antenna position) are completed, because:

$$\begin{cases} v_{x-ant} = v_{xy-ant} \cdot \cos(\psi - \varphi_{ant}) \\ v_{y-ant} = -v_{xy-ant} \cdot \sin(\psi - \varphi_{ant}) \end{cases}.$$

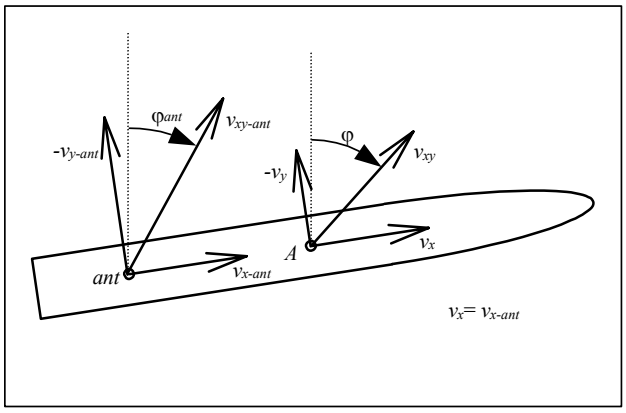

Fig.3. Antenna reduction

2.3. Antenna position reduction

As our reference system is fixed at midship ("A") position, it is required to convert relevant velocities according to the following formulas:

$$\begin{cases} v_x = v_{x-ant} \\ v_y = v_{y-ant} - \omega_z \cdot \Delta a \\ \omega_z = \omega_{z-ant} \end{cases}.$$

For the ship and manoeuvre under our investigation, the final midship-related velocities are presented in Fig. 4.

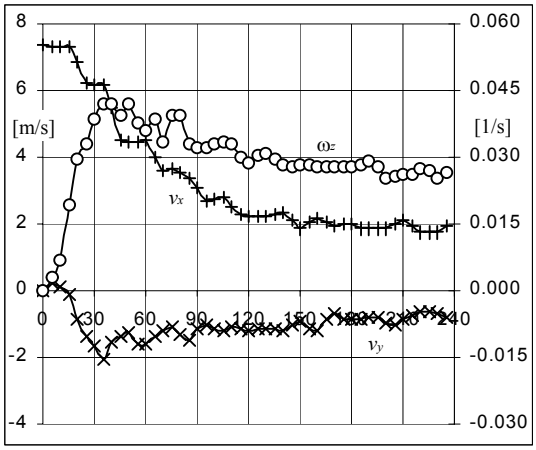

Fig. 4. Turning circle velocities

2.4. Accelerations identification

Differentiation of velocities calculated at the previous stage (2.2) leads to accelerations of the ship's body (Fig. 5), defined as:

$$a_x = \frac{dv_x}{dt}, \quad a_y = \frac{dv_y}{dt}, \quad \varepsilon_z = \frac{d\omega_z}{dt}.$$

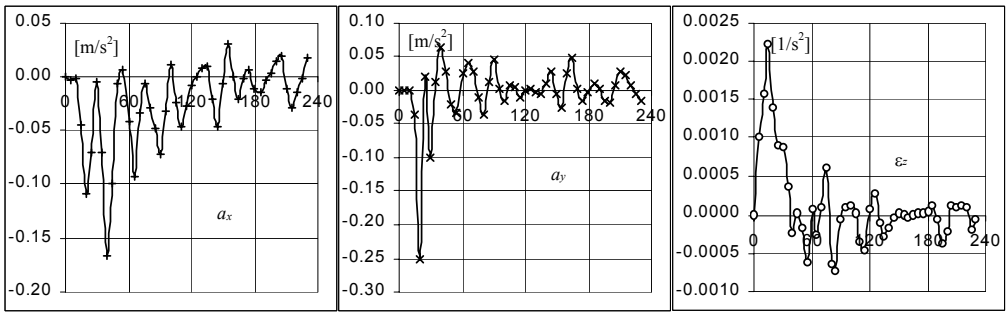

Fig. 5. Turning circle accelerations

2.5. Total force identification

Till now, all the results are not affected by any assumptions. Subsequent calculations need some guess, what leads to somehow assumptions-fouled data.

Estimating ship's moment of inertia J_z by using the non-dimensional radius of inertia for loaded bulk carrier (unpublished data, L/B=7.6, B/T=2.2), see Table 1, and taking added masses according to [Clarke et al., 1983], the following ratios are received (m_{11} - ellipsoid based):

$$\frac{m_{11}}{m} = 0.06, \quad \frac{m_{22}}{m} = 1.00, \quad \frac{m_{66}}{J_z} = 0.83 .$$

And now, directly from motions equations (3), external force components can be computed (Fig. 6).

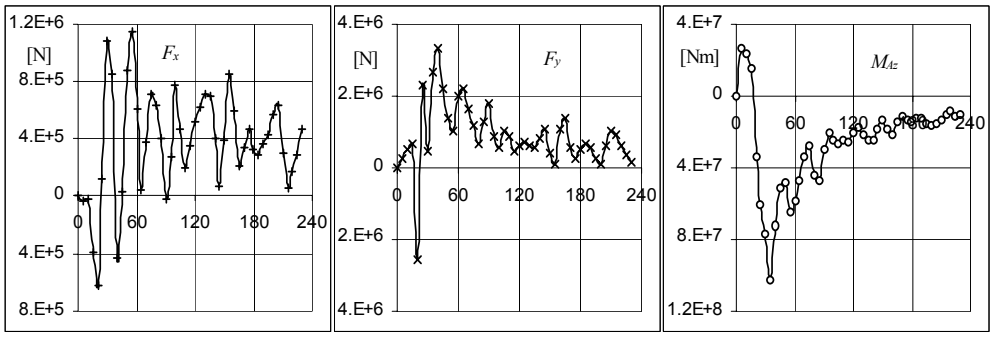

Fig. 6. Turning circle external total force components

Due to roughly estimated added masses, one should take into account their not negligible impact. Recalculating all force components, individually for each added masses changed ±50% around its initial value, some interesting conclusions can be drawn. The influence of surge added mass (m_{11}) is completely undetectable for any force component, thus it could be consider a "dead" parameter in the motion mathematical model. Yaw added mass (m_{66}), by the nature of set (3), could affect only a moment component (M_{Az}), but the change in the moment (Fig.7) is significant in the positive part only (time <20s, initial turn), where m_{66} higher +50% produces change in a moment +10%. Sway added mass (m_{22}) is absolutely the most important factor in creating an external force image (Fig. 7) in the whole time period: the great impact on F_x and M_{Az}, clearly smaller sense in F_y. Due to differentiation errors (1.2.), for purpose of Fig. 7 analysis, an averaging view must be applied.

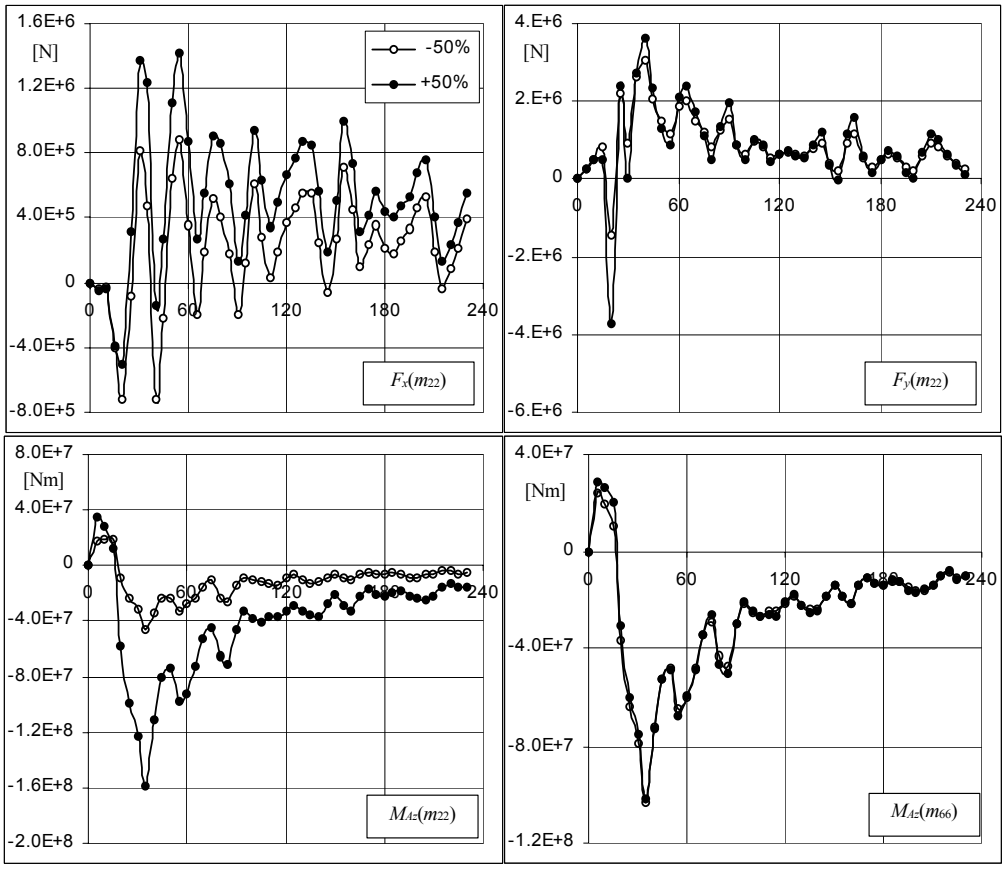

Fig. 7. Added masses effect on external force

Introducing a common modular model of total force i.e. being sum of hull (H), propeller (P) and rudder (R) sub-forces (with relevant interactions), in this case the main objective is to evaluate rudder (F_{xR}, F_{yR}) and hull components (F_{yH}, M_{AzH}) only:

$$\begin{cases} F_x = F_{xH} + F_{xP} + \underline{F_{xR}} \\ F_y = F_{yH} + F_{yP} + F_{yR} = \underline{F_{yH}} + \underline{F_{yR}} \\ M_{Az} = M_{AzH} + M_{AzP} + M_{AzR} = \underline{M_{AzH}} + M_{AzR} \end{cases} \tag{4}$$

Because, resistance (F_{xH}), propeller force (effective thrust, F_{xP}) and rudder moment (M_{AzR}), the latter as a product of rudder offset (negative) and rudder transverse force (F_{yR}), are generally well established in the literature.

The way to the solution leads from "rudder" towards "hull" (not oppositely). The reasons for such approach are:

- rudder hydrodynamics is mostly available (the form of c_L-lift and c_D-drag coefficients) and pretty accurate, though some difficulties arise, while acquiring data for untypical constructions and in case of different than assumed conditions; for tuning c_L-c_D characteristics - F_{xR} should be used,
- F_{xR} is directly identified from surge motion equation (3), but it needs very accurate sway added mass (m_{22}), what implies necessity of adjusting this roughly estimated parameter (i.e. when not integrated individually over the hull, as in our case) by means of F_{xR} guess,
- ship's hulls differ greatly and allow hardly for their regression analysis, particularly in the whole range of drift and yaw rate, individual experiments are highly costly.

2.6. Rudder longitudinal force determination

Taking propeller characteristics based on [Oosterveld et al., 1975] results, main engine overload controlled by revolutions decrease ([Artyszuk, 1997]), it is possible now to distribute total longitudinal force into its components (Fig. 8).

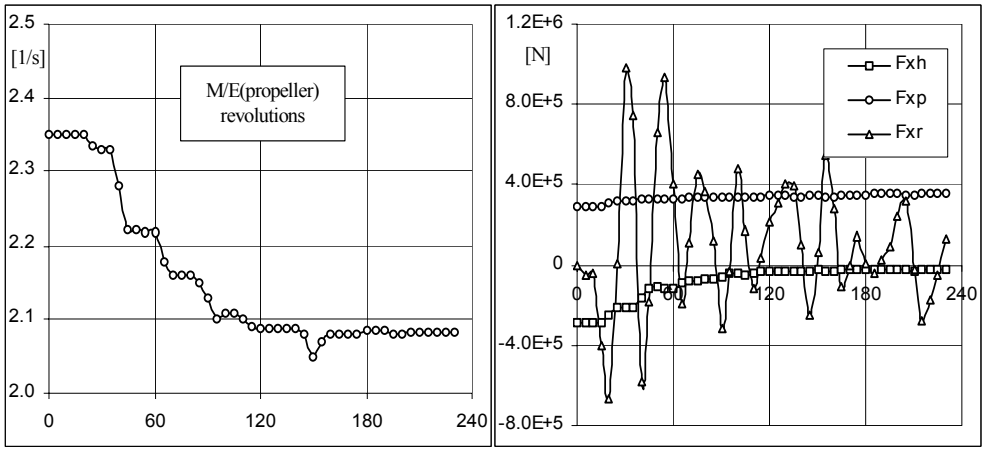

Fig. 8. Final decomposition of longitudinal force

Taking a closer look at the rudder phenomenon, it is evident that F_{xR} reaches maximum negative value just at the begin of turning (i.e. maximum inflow angle, negative value for starboard turn always), which tends to decrease to a steady level as the rudder local drift is increasing and stabilizing. But F_{xR} is generally negative in all time period, when the propeller slipstream area is considered, and the latter one is a sufficient approximation (dominant contribution) of the whole rudder behavior. Fig. 8. shows, instead of it, mostly positive trend of F_{xR}, which is not acceptable.

Fig. 9 denotes a change of incidence angle α_R according to two basic models existing in the literature:

- theoretically based - "A" (refer to e.g. [Oltmann et al., 1984]),
- semi-empirically related - "B" [Inoue et al., 1981].

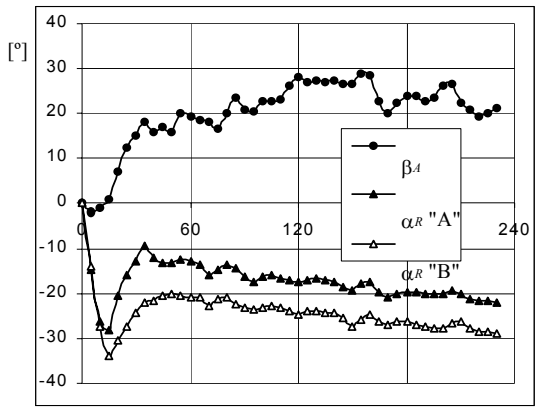

Fig. 9. Midship drift and simulation of rudder inflow angl (rudder deflection 35º)

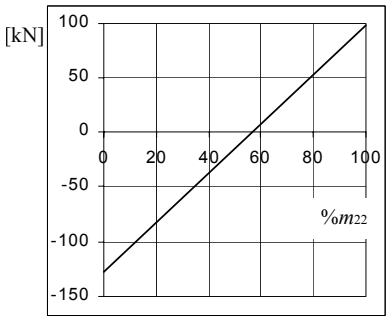

Fig. 10. Rudder longitudinal force as function of m_{22}

The average value of F_{xR} starting from 120 seconds (steady phase of circulation) is nearly +100kN. To achieve at least null F_{xR}, it is required to change m_{22} to 57% of its initial value. The dependence of discussed average F_{xR} on $\%m_{22}$ is of course linear. For convenience, this relationship is brought up in Fig. 10.

Though, F_{xR} is not linearly related to the inflow angle α_R, it seems to be very helpful for the final identification (fairing) of rudder forces, when we superimpose Fig.8 upon data of Fig. 9. This is demonstrated (Fig. 11) for F_{xR} relevant to $57\%m_{22}$ (null case) and $30\%m_{22}$ (middle case).

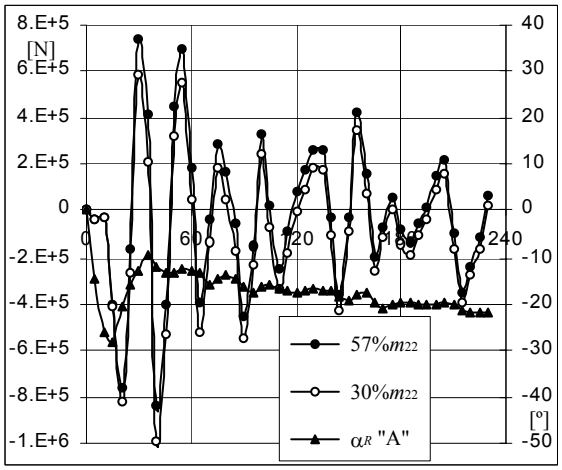

Fig. 11. F_{xR} - α_R superimposition

2.7. Rudder further remarks

In author's opinion, a proper evaluation of rudder longitudinal force should play a key role in the identification of other rudder force components. There are a few factors strongly affecting this process and needed to be available:

- smoothing of all curves contributing to the final calculation outcome (for accuracy and clarity),
- accurate added masses (single solution),
- basic data of untypical rudders (e.g. Schilling's type - our case),
- well acceptable model of rudder inflow.

2.8. Hull forces

Hull forces identification is the last task in the process. They are directly calculated from equations (4). The next step is to calculate non-dimensional coefficients (of any convenient form) of hull forces as function of drift angle (at midship position - β_A, see Fig. 9) and angular relative velocity (i.e. ω_z defined against v_{xy}) and store them as 2-dimensional tables.

All described steps ensure the complete identification of ship's dynamics.

Though the turning circle gives drift of about ±30 degrees and middle values of yaw rates, other tests could be processed in the same manner as specified in this paper with the objective to identify other areas of drift and angular velocity variation (whole range of their possible change).

CONCLUSIONS

The beforehand stated procedure needs completion of some additional steps (2.7) to be seen in full action for the ship investigated (Tab. 1). It points a real and easy way to identify the ship's dynamics of existing ships, which is supplied next to the ship motion mathematical model unit of different sophisticated integrated navigational systems. Besides this primary purpose, the scheme presented has one more advantage. Namely, it provides for means of evaluating quality of ship's trials. Such features show quickly an evidence, that some behavior can not be reached in any sensible status of model parameters (see case of m_{22} in p. 2.5). Those trials ought to be disregarded immediately.

BIBLIOGRAPHY

1. Artyszuk J. "General equations of ship's motion - a practical solving algorithm", (in Polish), ZN Nr 55, Maritime University, Szczecin 1998
2. Artyszuk J. "Low-level mathematical model of ship's surge motion", (in Polish), International Scientific and Technical Conference on Sea Traffic Engineering, Part I, Martitime University, Szczecin 1997.
3. Clarke D., Gedling P., Hine G. "The Application of Manoeuvring Criteria in Hull Design Using Linear Theory", RINA Trans. 1983.

4. Inoue S. et al. "A Practical Calculation Method of Ship Maneuvering Motion", ISP No.325 (Sep/1981).
5. Oosterveld M.W.C., Oossanen P. "Further Computer-Analyzed Data of the Wageningen B-Screw Series", ISP No.251 (Jul/1975).
6. Oltmann P., Sharma S.D. "Simulation of Combined Engine and Rudder Maneuvers Using an Improved Model of Hull-Propeller-Rudder Interactions", 15th Symposium on Naval Hydrodynamics, Hamburg Sep'84.
7. Ralston A. "A first course in numerical analysis", (Polish edition), PWN, Warsaw 1983.